Table 1 Stall warning time

% speed	Rotor 4, unswept	Rotor 6, backward swept
60	Progressive stall	Progressive stall
70	<0.10 s	Progressive stall
80	<0.10 s	0.2 s
90	0.35 s	>2.0 s
100	0.1 s	0.2 s

are attenuated through a shock structure rotating at blade passing frequency. Attenuation of rotating disturbances is less for the rotor designed for reduced tip shock strength (R6), and stall can be detected earlier in the process, as was the case for R6.

Summary

Two single-stage, transonic compressor designs were tested for the presence of modal wave development in the process leading up to aerodynamic stall. The two rotors had similar design points (speed, pressure ratio, mass flow) and were tested in the same rig under the same operating conditions. The stalling process of both transonic rotors was associated with the growth of small amplitude rotating waves (modal waves) for all speeds tested. Prestall time of emergence of the waves is believed to be correlated with the shape of the stage characteristic (speed line). In cases where the speed line slopes of the two rotors were virtually identical, the swept rotor (R6) exhibited more stall warning time than the unswept design, suggesting that reduced shock strength due to backsweep may favor advanced detection of the modal waves.

References

[1]Epstein, A. H., Ffowcs Williams, J. E., and Greitzer, E. M., "Active Suppression of Aerodynamic Instabilities in Turbomachines," *Journal of Propulsion and Power*, Vol. 5, No. 2, 1989, pp. 204–211.

[2]Paduano, J., Epstein, A. H., Valavani, L., Longley, J. P., Greitzer, E. M., and Guenette, G. R., "Active Control of Rotating Stall in a Low Speed Axial Compressor," American Society of Mechanical Engineers Paper 91-GT-88, June 1991.

[3]Day, I. J., "Active Suppression of Rotating Stall and Surge in Axial Compressors," American Society of Mechanical Engineers Paper 91-GT-87, June 1991.

[4]Badmus, O. O., Chowdhury, S., Eveker, K. M., Nett, C. N., and Rivera, C. J., "A Simplified Approach for Control of Rotating Stall, Part 1: Theoretical Development," AIAA Paper 93-2229, June 1993.

[5]Badmus, O. O., Chowdhury, S., Eveker, K. M., Nett, C. N., and Rivera, C. J., "A Simplified Approach for Control of Rotating Stall, Part 2: Experimental Results," AIAA Paper 93-2234, June 1993.

[6]McDougall, N. M., Cumpsty, N. A., and Hynes, T. P., "Stall Inception in Axial Compressors," *Journal of Turbomachinery*, Vol. 112, Jan. 1990, pp. 116–125.

[7]Garnier, V. H., Epstein, A. H., and Greitzer, E. M., "Rotating Waves as a Stall Inception Indication in Axial Compressors," American Society of Mechanical Engineers Paper 90-GT-156, June 1990.

[8]Hah, C., and Wennerstrom, A. J., "Three-Dimensional Flowfields Inside a Transonic Compressor with Swept Blades," *Journal of Turbomachinery*, Vol. 113, April 1991, pp. 241–251.

[9]Law, C. H., and Puterbaugh, S. L., "Parametric Blade Study Test Report Rotor Configuration No. 4," Air Force Wright Aeronautical Labs., AFWAL-TR-88-2110, Wright–Patterson AFB, OH, Nov. 1988.

[10]Day, I. J., "Stall Inception in Axial Flow Compressors," American Society of Mechanical Engineers Paper 91-GT-86, June 1991.

[11]Boyer, K. M., "Characterization of Stall Inception in High-Speed Single-Stage Compressors," M.S. Thesis, Air Force Inst. of Technology, AFIT/GAE/ENY/92D-21, Wright–Patterson AFB, OH, Dec. 1992.

[12]Greitzer, E. M., "Surge and Rotating Stall in Axial Flow Compressors," Pts. I and II, *Journal of Engineering for Power*, Vol. 98, April 1976, pp. 190–217.

[13]Bonnaure, L. P., "Modeling High Speed Multistage Compressor Stability," M.S. Thesis, Massachusetts Inst. of Technology, Dept. of Aeronautics and Astronautics, Cambridge, MA, Sept. 1991.

[14]Sellin, M. D., Puterbaugh, S. L., and Copenhaver, W. W., "Tip Structures in Transonic Compressor Rotors," AIAA Paper 93-1869, June 1993.

[15]Garnier, V. H., "Experimental Investigation of Rotating Waves as a Rotating Stall Inception Indication in Compressors," Gas Turbine Lab., Massachusetts Inst. of Technology, GTL Rept. 198, Cambridge, MA, Nov. 1989.

One-Dimensional, Equilibrium-Chemistry Ram Accelerator Performance Calculations

Federico Liberatore*
U.S. Army Research Laboratory,
Aberdeen Proving Ground, Maryland 21005-5066

Nomenclature

A = tube cross-sectional area
a = sound speed
F = thrust
H = assigned enthalpy
h = sensible enthalpy
M = Mach number
P = static pressure
q = heat
R = gas constant
T = temperature
U = velocity
v = specific volume
γ = specific heat ratio
ΔH_f = enthalpy of formation
ρ = density

Subscripts
1 = initial state
2 = final state

Superscripts
$*$ = Chapman–Jouget detonation velocity
$''$ = current iteration in Newton–Raphson numerical scheme
0 = reference temperature

Introduction

THE use of steady, equilibrium-chemistry, one-dimensional control-volume equations to analyze ram accelerator performance has been documented and good agreement between theory and experiment has been observed for successfully started projectiles operating in the subdetonative regime ($U < 0.85 \times U^*$).[1-4] The one-dimensional formulation does not permit detailed understanding of flowfield behavior inside the control volume, but does emphasize the important dimensionless groups useful in quantifying overall performance. The dimensionless groups are M, projectile thrust (F/AP_1), and energy release ($\Delta q/C_pT_1$). If finite rate kinetics

Received Jan. 14, 1995; revision received March 24, 1995; accepted for publication March 27, 1995.

*SCEEE Post Doctoral Engineering Fellow, Weapons Technology Directorate, Propulsion Branch, M/S AMSRL-WT-PA.

are assumed instead of equilibrium chemistry, then an additional dimensionless group representing the induction time of the mixture can be formed.

One-dimensional control-volume theory cannot predict a priori if a projectile geometry and gas mixture combination will work successfully. This must be done with a more sophisticated calculation such as computational fluid dynamics (CFD).[5] The results of CFD calculations and/or experiments can be used to define the performance envelope of the projectile in terms of the previously mentioned dimensionless groups. Once the performance envelope of a projectile has been defined, one-dimensional control volume theory can be used to screen potentially suitable gas mixtures. The primary motivation for this is to allow a fixed geometry to function at higher velocities using mixtures that have progressively higher sound speeds and comparable levels of energy release.

The NASA Lewis CET89 code is capable of calculating various one-dimensional, equilibrium-chemistry flows.[6] The CET89 code was modified to include one-dimensional ram accelerator performance calculations. The modified code efficiently calculates thrust curves for a given initial gas mixture and has full access to the original thermodynamic database.[7] This allows the reduction of data and evaluation of potential fuel mixtures to be done in a systematic manner. Application of the results of the computer program must be done so with the acknowledgment that the absence of kinetic effects can have serious implications for the performance of the projectile. The location of the energy release around the projectile is of vital importance to performance and is something that will change with different reactant gas mixtures.

Discussion

The governing equations for the one-dimensional ram accelerator are given by Eqs. (1–3):

$$\rho_1 U_1 = \rho_2 U_2 \qquad \text{continuity} \tag{1}$$

$$P_1 + \rho_1 U_1^2 + (F/A) = P_2 + \rho_2 U_2^2 \qquad \text{momentum} \tag{2}$$

$$H_1 + \tfrac{1}{2}U_1^2 = H_2 + \tfrac{1}{2}U_2^2 \qquad \text{energy} \tag{3}$$

Enthalpy is defined by Eq. (4):

$$H = \Delta H_f^0 + (h - h^0) \tag{4}$$

Following the derivation in Gordon and McBride,[6] the three governing equations are reduced to two by substituting continuity into momentum and energy which, along with the assumption that $M_2 = 1$ (thermally choked end state), results in Eqs. (5) and (6)[7]:

$$\frac{P_1}{P_2} = \frac{1 - \gamma_2[(\rho_2/\rho_1) - 1]}{1 + (F/AP_1)} \tag{5}$$

$$H_2 = H_1 + \tfrac{1}{2}\gamma_2 R_2 T_2[(\rho_2/\rho_1)^2 - 1] \tag{6}$$

Equations (5) and (6) are used to implement a Newton–Raphson iteration scheme to determine the final state of the process[6]:

$$P'' - (P_1/P_2) = 0 \tag{7}$$

$$H'' - H_2 = 0 \tag{8}$$

P'' and H'' are the current guesses at pressure and enthalpy and comparison with the right-hand sides of Eqs. (5) and (6), respectively, and they determine if convergence is achieved. Corrections for the current values of pressure and temperature are arrived at by solving the following set of two equations simultaneously[6]:

$$\frac{\partial[P'' - (P_1/P_2)]}{\partial\,\Delta(P_2/P_1)}\Delta\left(\frac{P_2}{P_1}\right) + \frac{\partial[P'' - (P_1/P_2)]}{\partial\,\Delta(T_2/T_1)}\Delta\left(\frac{T_2}{T_1}\right) = P'' - \frac{P_1}{P_2} \tag{9}$$

$$\frac{\partial[(H'' - H_2)/R]}{\partial\,\Delta(P_2/P_1)}\Delta\left(\frac{P_2}{P_1}\right) + \frac{\partial[(H'' - H_2)/R]}{\partial\,\Delta(T_2/T_1)}\Delta\left(\frac{T_2}{T_1}\right) = \frac{(H'' - H_2)}{R} \tag{10}$$

$\Delta(P_2/P_1)$ and $\Delta(T_2/T_1)$ are the two unknowns being solved for and represent corrections to the current guessed values of P_2 and T_2. The current values of P_2 and T_2 are used to calculate the coefficients and nonhomogeneous terms in Eqs. (9) and (10). Iteration stops when the corrections become sufficiently small ($<0.5 \times 10^{-4}$). The presence of the thrust parameter (F/AP_1) modifies the terms in Eq. (9), but has no influence on Eq. (10). Expanded expressions for the coefficients and nonhomogeneous terms in Eqs. (9) and (10) are given in Liberatore[7] and Gordon and McBride,[6] respectively. After the final state is determined, the energy released is calculated from the change in enthalpy of formation from reactants to products:

$$\Delta q = \Delta H_f^0|_1 - \Delta H_f^0|_2 \tag{11}$$

As a result of the chosen sign convention positive values of Δq denote exothermic reactions.

The inclusion of the parameter (F/AP_1) into the Hugoniot equations expands the final results by one dimension, from two discreet points to a line. The two endpoints are the Chapman–Jouget detonation and deflagration points and all of the intermediate points on the curve satisfy Chapman–Jouget constraints, with the exception of a thrust force being produced inside the control volume.

Figure 1 shows the result of a calculation plotted in the thermodynamic plane (pressure ratio vs specific volume ratio).

The thrust curve can be divided into two regions, the detonation branch and the deflagration branch. These two regions are divided by the maximum thrust point, which occurs when $(v_2/v_1) = 1$. In the classical Rankine–Hugoniot analysis that does not include the thrust parameter (F/AP_1), a solution along the line $(v_2/v_1) = 1$ is impossible because it implies M_2

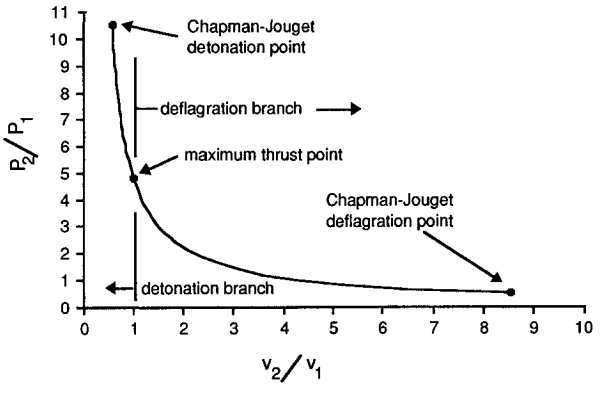

Fig. 1 Sample thrust curve plotted in the thermodynamic plane. Reactant mixture is $3CH_4 + 2O_2 + 10N_2$ at initial conditions P_1 = 51 atm, T_1 = 298 K.

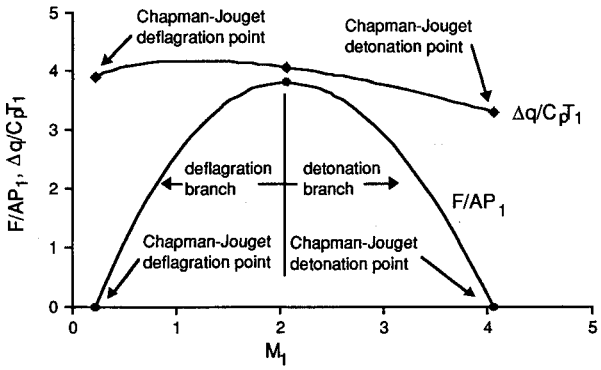

Fig. 2 Sample thrust curve plotted vs. velocity. Reactant mixture is $3CH_4 + 2O_2 + 10N_2$ at initial conditions $P_1 = 51$ atm, $T_1 = 298$ K.

$= \infty$. The presence of the thrust parameter causes the Rayleigh line to pass through the point

$$(v_2/v_1,\ P_2/P_1) = [1,\ 1 + (F/AP_1)]$$

shifting it closer to the Hugoniot curve. As the value of the thrust parameter is increased, the two respective solution points in the thermodynamic plane move closer to one another until the maximum thrust value is attained. At this point, the Rayleigh line can be tangent to the Hugoniot curve at only one point

$$(v_2/v_1,\ P_2/P_1) = [1,\ 1 + (F/AP_1)|_{\max}]$$

and the two solutions collapse to one.

Figure 2 shows the same calculation from Fig. 1, but it is plotted in terms of thrust and energy release as functions of velocity. Not shown in the plot are negative-valued solutions (net drag) that extend from both sides of the curve. The Chapman–Jouget deflagration is never observed in reality and the thrust curve in Fig. 2 provides an explanation for this. A perturbation away from the Chapman–Jouget detonation point will result in a force restoring it to the original velocity while a perturbation away from the Chapman–Jouget deflagration point will result in a force deflecting it further from the original velocity. It is assumed, by analogy, that some portion of the thrust curve near the Chapman–Jouget deflagration point will be physically unrealistic. A method for quantifying this region has not been developed, and so the thrust curve is shown in its entirety.

Conclusions

A quick and efficient method of calculating one-dimensional ram accelerator performance has been developed through modification of the NASA Lewis CET89 computer code. The modified program is best used for analyzing subdetonative ram accelerator propulsion and for evaluating prospective reactant mixtures. Caution has to be exercised when using the results of these calculations because reaction kinetics play a major role in the operation of the ram accelerator where combustion is premixed in nature. One-dimensional theory also fails to predict successful operation above the Chapman–Jouget detonation speed.

References

[1]Bruckner, A. P., Knowlen, C., Hertzberg, A., and Bogdanoff, D. W., "Operational Characteristics of the Thermally Choked Ram Accelerator," *Journal of Propulsion and Power*, Vol. 7, No. 5, 1991, pp. 828–836.

[2]Knowlen, C., and Bruckner, A. P., "A Hugoniot Analysis of the Ram Accelerator," 18th International Symposium on Shock Waves, Sendai, Japan, July 1991.

[3]Chew, G., Knowlen, C., Burnham, E. A., Hertzberg, A., and Bruckner, A. P., "Experiments on Hypersonic Ramjet Propulsion Cycles Using a Ram Accelerator," AIAA Paper 91-2489, June 1991.

[4]Higgins, A. J., Knowlen, C., and Bruckner, A. P., "An Investigation of Ram Accelerator Gas Dynamic Limits," AIAA Paper 93-2181, June 1993.

[5]Nusca, M. J., "Reacting Flow Simulation for a Large Scale Ram Accelerator," AIAA Paper 94-2963, June 1994.

[6]Gordon, S., and McBride, B. J., "Computer Program for Calculation of Complex Chemical Equilibrium Compositions, Rocket Performance, Incident and Reflected Shocks, and Chapman-Jouget Detonations," NASA SP-273, March 1976.

[7]Liberatore, F., "Ram Accelerator Performance Calculations Using a Modified Version of the NASA CET89 Equilibrium Chemistry Code," Army Research Lab. Technical Rept., ARL-TR-647, Dec. 1994.

Performance Comparisons of Low-Power Arcjets

W. D. Deininger,* G. Cruciani,† and M. J. Glogowski‡
BPD Difesa e Spazio, 00034 Colleferro, Rome, Italy

Introduction

ELECTRIC PROPULSION (EP) has recently attracted renewed attention in the space community due to the mass savings and/or payload increases it can provide to geostationary satellites. Although EP has been around for quite a long time, EP systems have been recognized as a mature technology for potential use in space only during the past several years. This is due to several factors. First, extensive EP test programs have not only improved the system performance, but have largely resolved the concerns related to EP integration and compatibility with the spacecraft. A second factor is the competition in the telecommunications satellite community, which pushes satellite subsystems towards higher performance to enhance the satellite capacity. In this sense, EP systems are attractive since they can offer launch mass reductions, increased on-orbit life, and/or payload mass increases that fully justify the development costs. Finally, power generation and storage systems that are now available onboard communications satellites can also provide the power/energy requirements of an EP system.

Two EP system technologies are presently under development in Europe for orbit maintenance of telecommunications satellites: 1) arcjets and 2) ion engines.[1] Low-power arcjets (1 kW-class) can offer substantial propellant mass savings with respect to chemical propulsion systems due to their higher specific impulse. In addition, arcjet systems have a lower dry mass and are less complex than ion engine systems, whereas ion engine systems, based on specific impulse considerations alone, typically provide a larger propellant mass reduction. Arcjet thrusters also minimize spacecraft integration difficulties with monopropellant or bipropellant chemical

Received Aug. 1, 1994; revision received Dec. 16, 1994; accepted for publication Dec. 23, 1994.

*Senior Scientist, Manager Electric Propulsion Laboratory. Corso Garibaldi 22. Senior Member AIAA.

†Physicist, Electric Propulsion Laboratory; currently at Via Bologna 18, 62010 Montecorsaro (MC), Italy.

‡Engineer, Electric Propulsion Laboratory; currently at Pennsylvania State University, Department of Aerospace Engineering, University Park, PA, 16802. Member AIAA.